Development of an acoustic levitation based contactless metrological apparatus: Applications to surface tension and viscosity measurements of low melting temperature Ga droplets

H. Strozyk, T. Quatravaux, P Chapelle, Jonathan Martens, Julien Jourdan

DEVELOPMENT OF AN ACOUSTIC LEVITATION BASED CONTACTLESS METROLOGICAL APPARATUS: APPLICATIONS TO SURFACE TENSION AND VISCOSITY MEASUREMENTS OF LOW MELTING TEMPERATURE Ga DROPLETS.

H. Strozyk[1], T. Quatravaux[2], P. Chapelle[2], J. Martens[2], J. Jourdan[2]

[1] Direction Générale de l'Armement, 60 bd Gén Martial Valin, 75015 Paris, FRANCE
[2] Institut Jean Lamour, Campus Artem, 2 allée André Guinier, 54011 Nancy, France

Keywords: Surface Tension, Viscosity, Acoustic Levitation, Gallium, Ni-based Superalloys.

Abstract

Aerospace engine efficiency is directly linked to the hot source temperature. Due to the very high temperature and mechanical stresses, turbine blades and discs have to be manufactured using alloys with exceptional high temperature properties. Nickel-based superalloys combine these properties. Conventional manufacturing processes are expensive, so manufacturers are promoting digital design methods. But numerical models rely on accurate thermophysical databases to be effectively representative of real processes. Due to the high chemical reactivity of molten nickel-based superalloys, viscosity and surface tension measurements are difficult. We have developed a non-contact metrological apparatus based on the acoustic levitation phenomenon, to perform these measurements on samples in liquid form. In order to develop this complex device, we have already carried out some measurements on water and low melting point Ga samples. This first phase of development has allowed us to identify improvements to be made in order to levitate high melting point reactive alloys.

Introduction

Thermodynamics is at the heart of open-cycle turbomachines used to propel modern aircrafts [1], [2]. First principle tells us that the higher the temperature difference between hot and cold sources, the more energy efficient the cycle. The most convenient mean to reach this goal is to increase the temperature of the hot source. But this leads to tremendous combined thermal and mechanical loads on parts, especially turbine blades and discs, running in these environments. Ni-based superalloys are particularly good at accommodating such constraints. On top of that, in order to reach mechanical performances required in aerospace engines, specific complex and expensive solidification processes, such as single crystal casting, must be used.
This leads to an ever more growing usage of numerical simulations to design these processes and predict their behavior [3]–[7]. But without accurate databases for fundamental material properties, such as surface tension, viscosity, density or thermal expansion for both solid and liquid states, numerical models are far less reliable for real processes description and control. These properties are not easily deduced from individual element characteristics, making it compulsory to perform specific measurements for each specific alloy.
Unfortunately, this type of alloy is highly reactive when taken into liquid state for elaboration purposes. To do so, chemically neutral environment, such as vacuum or inert gas atmosphere,

is needed. Also, lowering contact between samples and any solid surface, to prevent chemical pollution and parasitic interference regarding mechanical and solidification behaviors, is of paramount importance. These specifications are typically achieved by contactless methods such as levitation apparatus. Well-known and reliable techniques are ground or space-based electrostatic and magnetic levitation [8]–[11]. Nevertheless, to achieve perfect stability of levitated samples, they require complex regulated systems which are in the grasp of very few teams worldwide. Contrary to that, we developed a device based on acoustic levitation, which takes the advantage of acoustic standing waves to suspend high density samples in mid-air using quite passive systems.
In this work, we took advantage of water and Gallium samples, which are liquid at or close to room temperature, to train on measurement routes and to optimize our levitation system. Thanks to previous work [12], [13] and some theoretical considerations developed below, we try to demonstrate that the results obtained here for surface tension and viscosity of water and Ga samples, may help us to address measurements on high melting point reactive alloys, such as Ni-based superalloys.

Materials and Methods

Acoustic Levitation Device

We developed a levitating device, inspired by the work of Marzo and al. [14], later called the levitator, based on acoustic levitation technique. This method consists in the superposition of two acoustic waves producing a standing wave. The two original waves, which are travelling on the same path but in opposite directions, have same amplitudes and frequencies. This results in areas where time-averaged acoustic radiation pressure is either above or equal to ambient pressure. Locations of zero mean pressure amplitude variation are called nodes. These nodes are acoustic potential wells prone to trapping objects. The magnitude of this phenomenon can be numerically evaluated using Gork'ov potential [14]. Levitation and horizontal trapping efficiency are improved by arranging the piezoelectric ultrasound acoustic sources in hemispheres, forcing acoustic wave fronts to converge in a focal point. Our device is made of two hemispheres facing each other, comprised of fifty-height electrically connected in parallel 40 kHz emitters (ref.: Manorshi MSO-A1640HH10T) each, used to levitate samples. Piezo-buzzers are driven by a power system composed of a RS PRO RSDG 805 low frequency generator, supplying a driving low amplitude 40 kHz sinusoidal signal to an Audiophonics MA-CX02 linear amplifier. Hemispheres are driven π rad out of phase from each other. Output power is monitored and used to trim the acoustic pressure by using a RS PRO RSDM 3055A voltmeter in parallel with the whole levitator. Driving voltage is ranging from 3 to 40 V.

Materials

Initial studies were done using deionized water samples. This is done because heating while levitating is quite tricky and requires laser powered device to preserve the contactless interest of this kind of characterization techniques. Once levitated, the samples take the form of small droplets, more or less deviating from spherical shape, depending on the applied acoustic radiative pressure and gravity effect. Typical droplets volumes range from 2 to 10 µl.
Our ultimate goal is to achieve measurements on liquid metal. Because we don't have any appropriate heating mean yet, and as results discussed below on water droplets were quite satisfying, we then worked on molten Ga. This metal has a very low melting point of 29.8 °C

[15] which is near room temperature, making it suitable for preliminary tests. Knowledges acquired on water were supposed to be transferable on liquid metal, especially on Ga as melting point of both substances are quite close, compared to high melting point alloys. Relevance of this method is detailed in the Discussions section. Ga droplets are prepared by pumping preliminarily melted 99.999 % grade Ga (sourced from Aldrich Chem Co.) with a syringe and depositing them on a cool glass or metal surface. The quite good purity of the metal used induces a supercooling phenomenon, leaving droplets liquid even if substrate temperature is below Ga solidification point. This is overcome by touching the droplets with the stainless steel tip of the syringe, triggering their solidification.
Tests are made at room temperature and the temperature is monitored with a K type thermocouple (ref.: RS PRO IFC K T/C 1 mm x 0.25 m). Temperature is not controllable for the moment. As Ga tends to strongly oxidize under air, measurements are made inside a glove box filled with Ar gas (Air Liquide Ar Alphagaz 1 99.999 % purity).

Oscillating Droplets Measurement Methods

There are many different methods to perform measurements of thermophysical properties of high melting point materials [16], [17]. When using contactless devices as described in the Introduction section, oscillatory methods are the main tools. As far as acoustic levitation is concerned, several tentative have been successfully conducted on water at room temperature [18]–[20]. In parallel, different works have used oscillations to characterize liquid metals [8]–[10]. Two major techniques, namely the Freely Decaying (FD) oscillations method and the Frequency Response Function (FRF) technique, are used to measure viscosity and surface tension. These methods are largely based on Lamb and Lord Rayleigh theories of viscous oscillating spheres [21], [22].
FD method consists in applying a variable force, generally with an amplitude modulated sinusoidal shape at a given frequency, on the spherical liquid sample to be characterized. When shape oscillation is in a stationary state, the modulation is stopped. This allows the sphere to freely oscillate at its eigenfrequency while oscillation amplitude is being damped by viscous fluid flows. This phenomenon can be described by monitoring the shape of the droplet, especially its equivalent spherical radius, which may be expressed according to the following relationship:

$$R(t) = R_0 + A.\exp(-\tau t).\cos(2\pi f_0 t) \quad (1)$$

where $R(t)$ is the droplet instantaneous radius in m, R_0 is its radius at rest in m, A is the maximum amplitude of radius in m, τ is the oscillations damping constant in s^{-1}, t is the time in s and f_0 is the oscillations eigenfrequency in Hz. In this model, the droplet is supposed to be spherical, which is not the case in reality, as gravity and radiative acoustic pressure tend to flatten it. The droplet has an ellipsoidal shape. In equation (1) R_0 will thus be defined as the radius of the sphere of the same volume as the real droplet. Through data fitting procedures, this model can theoretically be used to simultaneously determine τ and f_0. Multiple parasitic frequencies are being present during experiments on water droplets, probably because of relatively low viscosity and imperfect stability of levitated samples. So we only use this model to determine τ. This reduces equation (1) to equation (2) when considering only raw signal envelope

$$R(t) = R_0 + A.\exp(-\tau t) \quad (2)$$

Figure 1 shows the typical pattern of a FD experiment on a water droplet. Droplet shape is captured using a high speed camera. For every instant of the experiment, an image processing algorithm is used to compute the surface area of the 2D projection of the droplet. One can see an oscillating stationary state at the beginning (0.0 to 1.1 s of experiment), corresponding to the period when the droplet oscillates under the action of the modulated acoustic pressure. A second period where the amplitude of the oscillations is progressively reduced is visible (1.1 s to end). This corresponds to the effective FD experiment when the forced oscillations are stopped. The droplet starts to oscillate following its eigenfrequency mode and the oscillations are damped as described before. Final state corresponds to the droplet at rest, its surface area being constant through time.

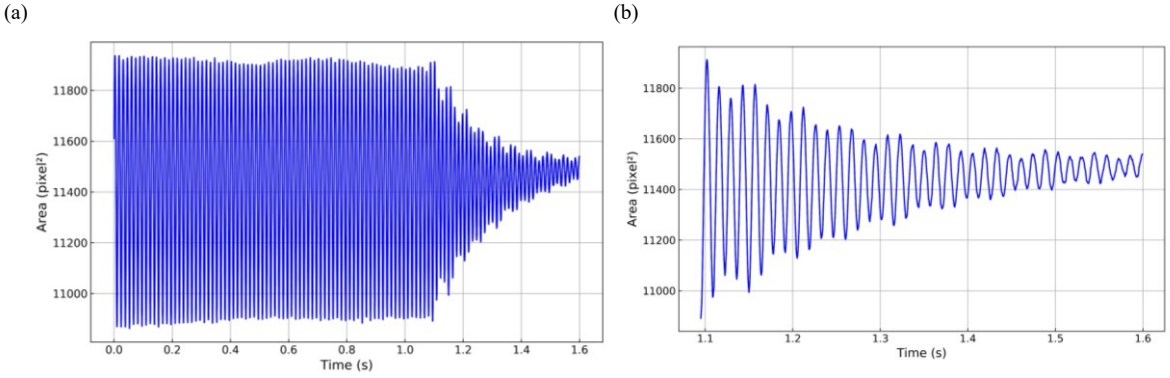

Figure 1. (a) Freely Decaying experiment on a 10 µl water droplet using a PHOTRON FASTCAM SA5 high speed camera, droplet surface versus time, 2000 images/s frame rate, 70 Hz modulation frequency, 2.5 % modulation amplitude, (b) focus on the oscillations damping time interval.

Further post-processing work is done with the raw signal shown on Figure 1, in order to be able to determine the damping constant. Figure 2 shows (a) the resulting signal when peaks of the envelope of the raw signal are identified and (b) the final state data when linear regression is performed on the log values of these peaks. The damping constant τ corresponds to the slope of the curve. Evaluations are performed using droplet area and not only equatorial or polar radius. This allows a measurement error reduction while equations (1) and (2) are still valid.
We then use images of the droplet at rest to perform a dimensional control. This provides accurate values for R_0, which is used in conjunction with τ to determine the dynamic viscosity of water droplets, using Lamb and Lord Rayleigh models given in equation (3):

$$\mu = \frac{\tau \rho R_0^2}{(l-1)(2l+1)} \quad (3)$$

Where l is the dimensionless degree of the Legendre polynomial used to model the shape of the 2D projection of the oscillating droplet and μ is the dynamic viscosity in $Pa.s$. The modulated acoustic pressure imposed on the droplets to drive their oscillations is applied in the vertical direction and mainly activate the fundamental oblate-prolate mode. This means that $l = 2$ and reduces equations (3) and (5) to equations (4) and (6).

Higher degree modes are less prone to be activated because of high energy and frequency required.

$$\mu = \frac{\tau \rho R_0^2}{5} \tag{4}$$

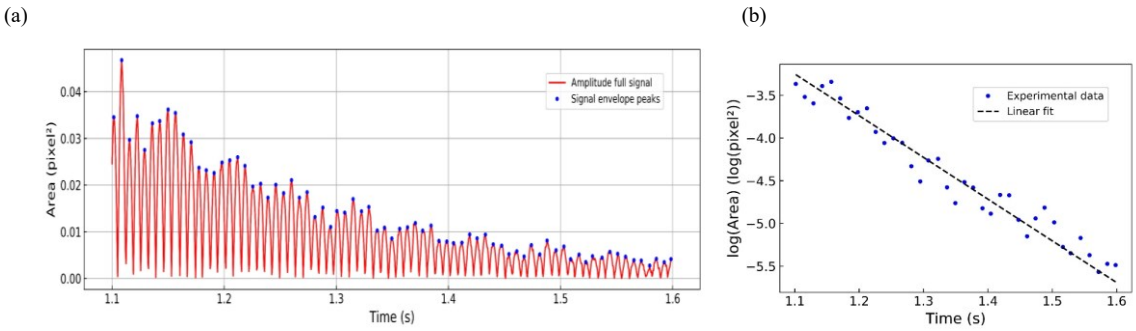

Figure 2. Post-processing of high speed camera data output, (a) droplet free oscillations envelope and (b) damping constant evaluation algorithm.

As discussed above, even if theoretically feasible, the use of FD experiment data to compute surface tension by using free oscillations eigenfrequency is quite tricky. In order to get this information, we performed FRF experiments. Figure 3 shows typical results on a water droplet.

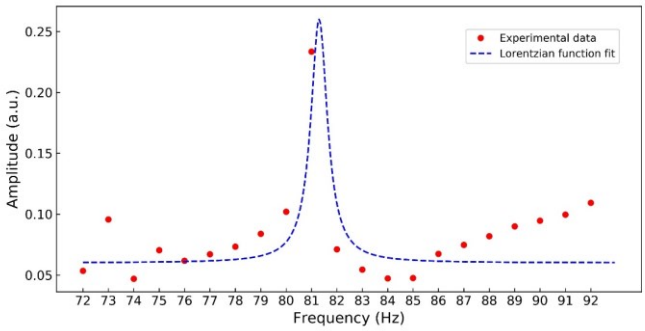

Figure 3. Frequency Response Function experiment performed on a 9 µl water droplet with shadowscopy setup, 72 to 92 Hz modulation frequency sweep with 1 Hz steps, 1.0 % amplitude modulation. Theoretical eigenfrequency is 81.7 Hz, measured is 81.4 Hz.

A FRF experiment consists in modulating the acoustic pressure on the samples the same way as explained for FD technique. However, forced oscillations are not released, but modulation frequency is swept over a range in which the theoretical eigenfrequency is supposed to be found. Mean amplitude of the oscillations is computed and correlated with modulation frequency. Frequency where amplitude is at its maximum is considered as eigenfrequency. Equations (5) and (6) then allow to evaluate surface tension:

$$\sigma = \frac{\rho (2\pi f_0)^2 R_0^3}{l(l-1)(l+2)} \tag{5}$$

$$\sigma = \frac{\rho(2\pi f_0)^2 R_0^3}{8} \quad (6)$$

Where σ is the surface tension in $N.m^{-1}$ and f_0 is the measured eigenfrequency in Hz. The FRF experiment were performed using an alternative technique to high speed camera. It is called "shadowscopy". It consists in illuminating the sample with a telecentric light source, which essentially means that light rays are almost parallel when hitting the droplets. The projected shadow of the sample is then observed using a photodiode. The luminous signal is converted in an electrical signal by the diode. When the droplet is at rest, a mean voltage level is given as an output signal. During FRF experiments, the surface oscillations of the droplet are transduced in voltage oscillations. FD experiments have also been performed using this setup. General trends are quite equivalent to high speed imaging but shadowscopy have some advantages, especially on accuracy, that will be considered in the Results and Discussions section. Because a protective atmosphere is needed for experiments on Ga samples, only high speed camera setup, which can be placed outside of the glove box, was used. Indeed, at the moment when tests were conducted, shadowscopy setup was not implemented inside the box.

Results and Discussions

High speed camera technique was the first approach used to measure viscosity. It is interesting because with reasonable post-processing development it can supply quite rich sets of data. Especially, we are able to determine at each instant of the experiments R_p and R_e which are respectively the polar and equatorial radii of the ellipse 2D projection of the droplets surface area. This allows us to determine the R_0 radius and use the models presented earlier. This also helps us to analyze the impact of the deviation to sphericity of the samples on the viscosity measurement accuracy. We also evaluated Ohnesorge number Oh, which represents a criterion for determining the applicability of the models to our samples. Kremer et al. [19] indicate that Oh should be lower than 0.1, which is the case for all of our experiments. Over the four considered trials, mean viscosity is equal to 1.431 $mPa.s$, which represents 43 % of error compared to the previous literature reference value of 1.0 $mPa.s$ at room temperature. Nevertheless, the order of magnitude is respected, despite the fact that uncertainty evaluation is not available for now. Limitation of high speed imaging is its inaccuracy when trying to further reduce the modulation amplitude. Too small oscillations cannot be captured and data are no longer exploitable. Indeed droplets oscillations cannot be identified among the background noise. On the other hand, quality of data fitting improves when acoustic radiative pressure increased. But as this tends to flatten the droplets, their geometry deviates from theoretical model hypothesis and thus error on viscosity also increases. Even if image processing provides a qualitative comprehension to how the droplets behave during experiments, it is unable to provide the required accuracy to reach metrological quality.

That's why we moved to shadowscopy. The sensitivity of the technique to small movements allows us to analyze smaller samples with lower modulation amplitudes. Results achieved with shadowscopy on intermediate size samples with important modulation amplitude are similar to those obtained with high speed camera. Mean viscosity is 1.220 $mPa.s$, which corresponds to 22 % of error with literature reference. But when volumes of around 2 µl are reached, viscosity measurement error starts to decrease significantly while still having satisfying oscillations

damping behavior. Considering the available results, mean viscosity is 1.020 $mPa.s$, lowering the relative error to only 2 %. The improvement of the quality of the results might be explained by the greater sphericity of the droplets under the action of surface tension and large reduction of parasitic macroscopic deformations because of small size. Nonetheless, as shadowscopy doesn't provide geometry information on the droplets, it is compulsory to take droplet geometry calibration pictures to perform calculations for viscosity evaluation.

Complementary results for surface tension on water were obtained using shadowscopy. Levitation configuration is quite similar to FD experiments. The volumes of the tested water samples are comprised between 8 and 10 µl. Average measured surface tension over seven experiments is 70.2 $mN.m^{-1}$, which corresponds to 2.5 % absolute error with respect to literature reference of 72 $mN.m^{-1}$. Some of the trials show two FRF peaks. After analysis, each of them can be identified as evolutive resonance because of droplet evaporation throughout the experiment duration, which is approximately 100 s (5 s recording for each frequency step).
Results are quite satisfying even if massive testing would be necessary to improve reproducibility and accuracy, by averaging measurement results.
A major conclusion of precedent experiments is that reducing the volume, thus approaching sample sphericity, and lowering modulation amplitude largely improve the measurements quality, in agreement with the conclusions of Kremer et al. [19] and Hosseinzadeh and Holt [20].

These results and know-hows being consolidated on quite easy access room temperature water measurements, transferability to liquid metal is now considered. In order to validate assumptions used for water, we worked on liquid Ga. We used the same methods and tools used for water. Ga is liquid nearly at room temperature, contrary to other metals tested in [15], [23]. As we don't have any powerful heating source compatible with acoustic levitation (i.e. induction heating or laser), using a simple IR lamp was enough to melt Ga samples while levitated. Weak power of this heating source prevent molten Ga to significantly exceed its melting point θ_f. Meaning viscosity can be considered quite equivalent to that at melting point.
Figure 4 introduces typical results obtained on Ga samples with high speed camera monitoring. Oblate-prolate oscillations are clearly visible on Figure 4.a time-lapse. Near-resonance modulation is quite tricky because it is prone to easily trigger undesired oscillation modes such as "rocking" and rotation. That is why we performed our FD experiments with a frequency shift with respect to resonance. Note that for the first tests on Ga, modulation amplitude was set relatively high compared to that used for water, in order to distinguish forced oscillations from background noise. In figure Figure 4.b, we were able to monitor polar radius R_p oscillations damping with a τ of 2.2 s^{-1}, which corresponds to a dynamic viscosity μ of approximately 3.05 mPa.s, given the R_0 radius of 1.06 mm of the considered sample. This result is quite promising when compared to the first results on water and improvements made later on. The viscosity value is in the appropriate order of magnitude. 56 % shift to 1.95 mPa.s literature value might be explained by the shift in modulation frequency explained above. Indeed, mechanical impedance of the droplet equivalent oscillator is higher when modulating away from resonance. Consequently, over-damping is faced and effective viscosity is greater than that at resonance.
Improvements may be achievable by reducing modulation amplitude, in order to prevent parasitic oscillations and thus allow measurement exactly on resonance.

(a) (b)

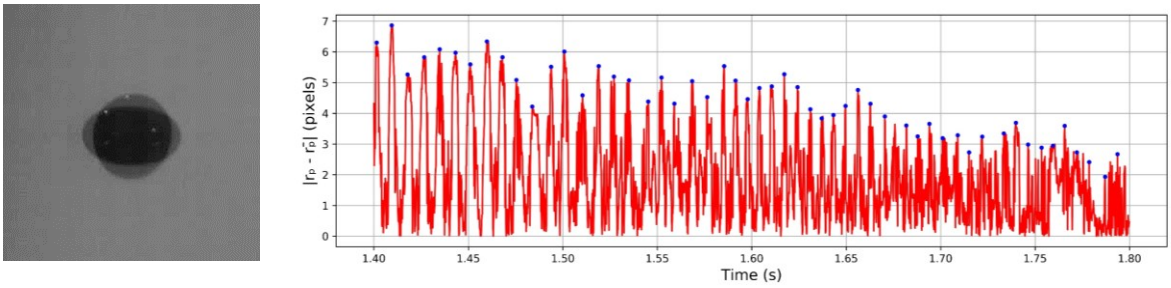

(c)

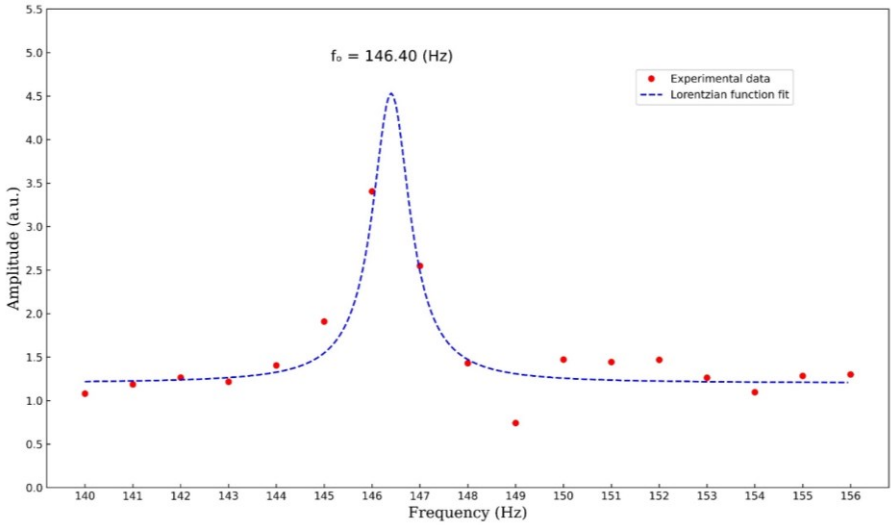

Figure 4.(a) Ga droplet oscillation time-lapse, (b) FD experiment on 1.06 mm R_0 radius droplet at 120 Hz modulation frequency and 10 % amplitude, (c) FRF experiment on 1.04 mm R_0 radius droplet with a 1 Hz modulation frequency step at 1.5 % amplitude.

Figure 4.c shows typical results obtained when performing FRF experiments. Important oscillation amplitude increase is detected when sweeping forcing frequency around theoretical resonance at 145.5 Hz. This was done using a 1 Hz step between 140 and 156 Hz. Using a Lorentzian function fitting model like [9], we were able to forecast a resonance frequency of about 146.4 Hz. Given the 1.04 mm R_0 radius of that particular sample, measured surface tension is 716.3 mN.m^{-1}, which corresponds to a 1.17 % shift from typical literature value of approximately 708 mN.m^{-1} [23]. As surface tension variation with temperature is quite small, even if temperature control is not achieved for the moment, we are quite confident concerning surface tension measurements. Improvements can still be made regarding two particular points. First, sampling step shall be reduced in order to more precisely identify resonance, thus improving surface tension accuracy. As FRF measurements are done “on the fly” while constantly increasing the forcing frequency every second during a 17 s time period, dynamic parasitic movements during frequency transitions may reduce measurement quality. Stabilization between steps could help overcome that issue. Then, oxygen management must be improved. O_2 concentration in the protective atmosphere has to be further reduced. Nevertheless, during development process to achieve measurements on Ga, we introduced a purifying system of the Ar supply, which led to O_2 concentrations of about 1.10^{-12} ppm. On top of that, Ga is quite reactive to oxygen present in the atmosphere during samples preparation.

So we also developed a process to remove Ga_2O_3 oxide by acid pickling before levitating samples.

Even if not straightforward, applicability of methods and measurement tools to Ga and consequently to higher melting point reactive alloys seem to be consolidated. Especially, FD and FRF techniques developed on water and efforts put to improve atmosphere cleanliness on Ga seem to open a promising path for Ni-based superalloys characterization.

Conclusions

The surface tension and viscosity of water and liquid Ga were investigated by the oscillating droplet method using an innovative acoustic levitation device. Good agreement with previous literature using different characterization methods, such as electromagnetic or electrostatic levitation, was obtained. Critical points to improve measurement accuracy are reducing samples size and modulation amplitude, which implies using more sensitive measurement methods such as shadowscopy. Better oxygen management in the atmosphere control box is also needed to prevent oxide deposition, introducing parasitic behaviors during oscillations.
Results obtained are quite encouraging for future developments on high melting point reactive alloys, such as Ni-based superalloys for aerospace applications. Given the sheer simplicity of acoustic levitation compared to previous techniques used for such characterizations, it is possible to envisage the development of a wider user community in the future.

Acknowledgments

We thank our industrial sponsors ArcelorMittal, Aperam Alloys, Vallourec, Eramet and Safran for their financial donation to the industrial chair Liquid Metal, which allows it to develop the present activity. We are also grateful to Métropole du Grand Nancy for its financial support. The French Ministry Of Defence, through the Direction Générale de l'Armement, is particularly thanked for its financial and technical support.

References

[1] M. Durand-Charre, *The Microstructure of Superalloys*. Grenoble: Publishers, Gordon and Breach Science, 1997.
[2] R. Reed, *The Superalloys, Fundamentals and Applications*, Cambridge. 2006.
[3] H. Combeau, M. Založnik, S. Hans, and P. E. Richy, "Prediction of macrosegregation in steel ingots: Influence of the motion and the morphology of equiaxed grains," *Metall. Mater. Trans. B Process Metall. Mater. Process. Sci.*, vol. 40, no. 3, pp. 289–304, 2009, doi: 10.1007/s11663-008-9178-y.
[4] L. Heyvaert, M. Bedel, M. Založnik, and H. Combeau, "Modeling of the Coupling of Microstructure and Macrosegregation in a Direct Chill Cast Al-Cu Billet," *Metall. Mater. Trans. A Phys. Metall. Mater. Sci.*, vol. 48, no. 10, pp. 4713–4734, 2017, doi: 10.1007/s11661-017-4238-z.
[5] A. Kumar, M. Založnik, H. Combeau, G. Lesoult, and A. Kumar, "Channel segregation during columnar solidification: Relation between mushy zone instability and mush permeability," *Int. J. Heat Mass Transf.*, vol. 164, p. 120602, 2021, doi: 10.1016/j.ijheatmasstransfer.2020.120602.
[6] J. Madison, J. Spowart, D. Rowenhorst, L. K. Aagesen, K. Thornton, and T. M.

Pollock, “Modeling fluid flow in three-dimensional single crystal dendritic structures,” *Acta Mater.*, vol. 58, no. 8, pp. 2864–2875, 2010, doi: 10.1016/j.actamat.2010.01.014.
[7] H. Zhang, Q. Xu, and B. Liu, “Numerical simulation and optimization of directional solidification process of single crystal superalloy casting,” *Materials (Basel).*, vol. 7, no. 3, pp. 1625–1639, 2014, doi: 10.3390/ma7031625.
[8] Y. Su *et al.*, “The relationship between viscosity and local structure in liquid zirconium via electromagnetic levitation and molecular dynamics simulations,” *J. Mol. Liq.*, vol. 298, 2020, doi: 10.1016/j.molliq.2019.111992.
[9] M. Mohr, R. K. Wunderlich, and H. J. Fecht, “Surface tension, viscosity and specific heat capacity of Ni-based superalloys MC2, LEK94 and CMSX-10 in the liquid phase measured in the Electromagnetic Levitator (EML-ISS) on board the international space station,” in *Proceedings of the Liquid Metal Processing & Casting Conference 2019*, 2019, p. 571, [Online]. Available: https://www.tms.org/LMPC2019%0Ahttps://drive.google.com/open?id=1_L0_QAe4d-6RqCPtSKjSAW9o9IqFRXoQ.
[10] M. Watanabe *et al.*, “Density, surface tension, and viscosity of Co-Cr-Mo melts measured using electrostatic levitation technique,” *Thermochim. Acta*, vol. 710, p. 179183, 2022, doi: 10.1016/j.tca.2022.179183.
[11] H. Yoo, C. Park, S. Jeon, S. Lee, and G. W. Lee, “Uncertainty evaluation for density measurements of molten Ni, Zr, Nb and Hf by using a containerless method,” *Metrologia*, vol. 52, no. 5, pp. 677–684, 2015, doi: 10.1088/0026-1394/52/5/677.
[12] Z. Y. Hong, W. J. Xie, and B. Wei, “Acoustic levitation with self-adaptive flexible reflectors,” *Rev. Sci. Instrum.*, vol. 82, no. 7, p. 074904, Jul. 2011, doi: 10.1063/1.3610652.
[13] B. Wei, “Levitation of Iridium and Liquid Mercury by Ultrasound ¨ ,” *Phys. Rev. Lett.*, pp. 1–4, 2002, doi: 10.1103/PhysRevLett.89.104304.
[14] A. Marzo, A. Barnes, and B. W. Drinkwater, “TinyLev: Supplementary,” *Rev. Sci. Instrum.*, vol. 88, no. 8, p. 085105, 2017, [Online]. Available: http://aip.scitation.org/doi/10.1063/1.4989995.
[15] D. Lucas and L. Lucas, “Viscosité des principaux métaux et métalloïdes,” *Tech. l’ingénieur*, vol. 33, no. 0, 1984.
[16] J. J. Li, “STUDY OF LIQUID METALS Thesis by John Jian-Zhong Li,” vol. 2009, 2009.
[17] Y. Y. Chang, M. Y. Wu, Y. L. Hung, and S. Y. Lin, “Accurate surface tension measurement of glass melts by the pendant drop method,” *Rev. Sci. Instrum.*, vol. 82, no. 5, 2011, doi: 10.1063/1.3587621.
[18] J. Arcenegui-Troya, A. Belman-Martínez, A. A. Castrejón-Pita, and J. R. Castrejón-Pita, “A simple levitated-drop tensiometer,” *Rev. Sci. Instrum.*, vol. 90, no. 9, 2019, doi: 10.1063/1.5096959.
[19] J. Kremer, A. Kilzer, and M. Petermann, “Simultaneous measurement of surface tension and viscosity using freely decaying oscillations of acoustically levitated droplets,” *Rev. Sci. Instrum.*, vol. 89, no. 1, 2018, doi: 10.1063/1.4998796.
[20] V. Ansari Hosseinzadeh and R. G. Holt, “Finite amplitude effects on drop levitation for material properties measurement,” *J. Appl. Phys.*, vol. 121, no. 17, 2017, doi: 10.1063/1.4982908.
[21] H. Lamb, “On the Oscillations of a Viscous Spheroid,” *Proc. R. Soc.*, no. 2, 1881.
[22] Lord Rayleigh, “On the Capillary Phenomena of Jets,” no. 05/05, 1879.
[23] N. Eustathopoulos, “Tension superficielle des métaux liquides et capillarité,” vol. 33, no. 0, 2017.